Neuron, Vol. 36, 451–461, October 24, 2002, Copyright ©2002 by Cell Press

Activity-Dependent Regulation of HCN Pacemaker Channels by Cyclic AMP: Signaling through Dynamic Allosteric Coupling

Jing Wang,[1,6] Shan Chen,[2,6] Matthew F. Nolan,[3] and Steven A. Siegelbaum[2,3,4,5]
[1]Integrated Program in Cellular, Molecular, and Biophysical Studies
[2]Department of Pharmacology
[3]Center for Neurobiology and Behavior
[4]Howard Hughes Medical Institute
Columbia University
722 West 168 Street
New York, New York 10032

Summary

Signal transduction in neurons is a dynamic process, generally thought to be driven by transient changes in the concentration of second messengers. Here we describe a novel regulatory mechanism in which the dynamics of signaling through cyclic AMP are mediated by activity-dependent changes in the affinity of the hyperpolarization-activated, cation nonselective (HCN) channels for cAMP, rather than by changes in cAMP concentration. Due to the allosteric coupling of channel opening and ligand binding, changes in cellular electrical activity that alter the opening of the HCN channels modify the binding of static, basal levels of cAMP. These changes in ligand binding produce long-lasting changes in channel function which can contribute to the regulation of rhythmic firing patterns.

Introduction

Recent experiments have enhanced our view of signaling through the classic second messenger cAMP. The identification of local protein signaling complexes (Bhalla and Iyengar, 1999; Davare et al., 2001; Marx et al., 2002; Michel and Scott, 2002) and subcellular compartments (Karpen and Rich, 2001; Zaccolo and Pozzan, 2002) has shown how a ubiquitous messenger can achieve spatial specificity. Our understanding of cAMP signaling has been broadened to include novel targets other than PKA, including the cyclic nucleotide-gated (CNG) (Zagotta and Siegelbaum, 1996) and hyperpolarization-activated HCN channels (Gauss et al., 1998; Ludwig et al., 1998; Santoro et al., 1998). However, one prevalent assumption, since the pioneering studies of Sutherland and colleagues (Robison et al., 1971), is that the dynamics of information transfer through the cAMP signaling cascade are driven by transient changes in the concentration of cAMP, generally as a result of changes in the concentration of an external ligand. Here we show how constant, nanomolar levels of basal cAMP give rise to a slow kinetic component in the voltage gating of the HCN channels through the allosteric coupling of channel opening to cAMP binding. Moreover, this process imparts a long-lasting, activity-dependent memory to HCN channels that underlies slow integrative changes in neuronal electrical activity.

The HCN channels are encoded by a family of four related genes, HCN1–4, which are members of the voltage-gated channel superfamily, with a membrane topology similar to a voltage-gated K^+ channel subunit (Santoro and Tibbs, 1999; Kaupp and Seifert, 2001). However, unlike most voltage-gated channels, the HCN channels are activated by hyperpolarization rather than depolarization. Additionally, the four HCN members all contain a conserved, 120 amino acid cyclic nucleotide binding domain (CNBD) in their cytoplasmic carboxy terminus. The direct binding of cAMP to the CNBD (DiFrancesco and Tortora, 1991) facilitates the activation of the HCN channels by removing an inhibitory influence of the CNBD on voltage gating (Wainger et al., 2001), shifting the voltage dependence of HCN gating to more positive potentials and speeding the rate of channel activation. This action of cAMP contributes to the increase in heart rate by autonomic signaling (DiFrancesco, 1993) and the alteration of neuronal firing patterns by modulatory synaptic inputs (Pape, 1996).

Previous studies showed that the modulation by cyclic nucleotides of steady-state gating of both the voltage-independent cyclic-nucleotide-gated channels (Goulding et al., 1994; Tibbs et al., 1997) and the voltage-gated HCN channels (DiFrancesco, 1999) could be explained by a cyclic allosteric model (Monod et al., 1965). According to this model, channel opening is allosterically coupled to a conformational change in the CNBD that enhances the affinity of the channel for ligand. The enhanced interaction of ligand with the open channel provides coupling energy that stabilizes the ligand-bound channel in the open state. For the hyperpolarization-activated HCN channels, the enhanced gating is manifest as a shift in the activation curve toward more positive potentials. Although the cyclic allosteric model provides a plausible mechanism for ligand gating, there have been few direct tests of the central hypothesis of the model that channel opening is allosterically coupled to enhanced ligand binding.

Here we provide qualitative and quantitative evidence that supports the notion of allosteric coupling by testing a previously unexplored prediction of the cyclic allosteric model: low concentrations of cAMP should induce a novel, slow kinetic component of channel opening in response to hyperpolarizing voltage steps. This slow phase of opening is predicted to result from the selective binding of low concentrations of cAMP to the high-affinity, open state of the channel, causing a slow conversion of channels from the ligand-free, closed state to the ligand-bound, open state during prolonged hyperpolarizations. We have confirmed this prediction and have shown that the properties of the slow component of activation are in quantitative agreement with the cyclic allosteric model. Moreover, we found that a slow kinetic component of HCN channel activation in resting cells results from the allosteric conversion due to binding of nanomolar levels of basal cAMP. Finally, the enhanced binding of cAMP to the open state endows HCN chan-

[5]Correspondence: sas8@columbia.edu
[6]These authors contributed equally to this work.

nels with an activity-dependent memory that leads to long-lasting changes in cellular excitability, which are likely to contribute to the generation of slow rhythmic firing patterns in certain regions of the brain.

Results

A Slow Phase of HCN Channel Opening Induced by Low Concentrations of cAMP

We have focused our studies on HCN2, an isoform expressed widely in brain and heart that shows a robust response to cAMP (Ludwig et al., 1998; Santoro et al., 2000; Chen et al., 2001). As noted previously, a high concentration of cAMP (≥10 μM) accelerates the rate at which the hyperpolarization-activated current (I_h) turns on during negative voltage steps (Figure 1A) and shifts the voltage dependence of activation to more positive potentials (Figure 1B). We now show that a low concentration of cAMP induces a novel, slow phase of channel activation (Figure 1A). In response to a hyperpolarization in the presence of 10 nM cAMP, the early time course of I_h activation is identical to that observed in the absence of cAMP. After a few hundred milliseconds, however, the activation time courses diverge, with the low concentration of cAMP inducing an additional slow increase in I_h magnitude.

As mentioned above (see Introduction), these results are consistent with the predictions of the cyclic allosteric model (Figure 1C). Thus, in the absence of cAMP, unliganded closed channels (C) enter the open state (O) in response to a hyperpolarizing voltage step through the nonfacilitated voltage-gated reaction pathway (C ↔ O). At high concentrations, cAMP will bind to the low-affinity, closed state of the channel prior to the hyperpolarization. As a result, during a hyperpolarization, these cAMP-bound channels will open rapidly and completely through the facilitated voltage-gated reaction pathway (AC ↔ AO). In contrast, in the presence of concentrations of cAMP that are too low to bind to the closed, low-affinity state of the channel, the unliganded channels will initially open in response to a hyperpolarization by the nonfacilitated voltage-gated reaction pathway (C ↔ O). This explains why the time courses of I_h activation in the absence of cAMP and in the presence of a low concentration of cAMP overlap initially. However, once unliganded channels open in the presence of cAMP, they will tend to bind ligand due to the enhanced affinity of the open state (A + O ↔ AO). This depletes the concentration of channels in the open, unliganded state, causing a reequilibration of channels from the closed, unliganded state to the open, liganded state, and produces the slow phase of channel opening (C → A + O → AO).

Kinetic Analysis of I_h Confirms Predictions of Cyclic Allosteric Model

To test more thoroughly the predictions of the cyclic allosteric model, we examined activation kinetics over a range of voltages for a range of cAMP concentrations. In the absence of cAMP, HCN2 channels in cell-free patches activate upon hyperpolarization with a time course that is well fit by a single exponential function (after an initial delay) (see Experimental Procedures), presumably reflecting the kinetics of the nonfacilitated, voltage-gated reaction for unliganded channels (Figure 2A). As the membrane is hyperpolarized to increasingly negative voltages, the exponential time constant of activation decreases from ~3 to ~1 s (Figures 2A and 3A). Attempts to fit the data with two exponential functions either failed to converge or did not yield a substantial improvement in the goodness-of-fit over a single exponential function (determined by χ^2, Figure 2D; see Experimental Procedures). We thus conclude that HCN2 currents are adequately described by a single exponential function.

In contrast to the single exponential kinetics of HCN2 in the absence of cAMP, two exponential components

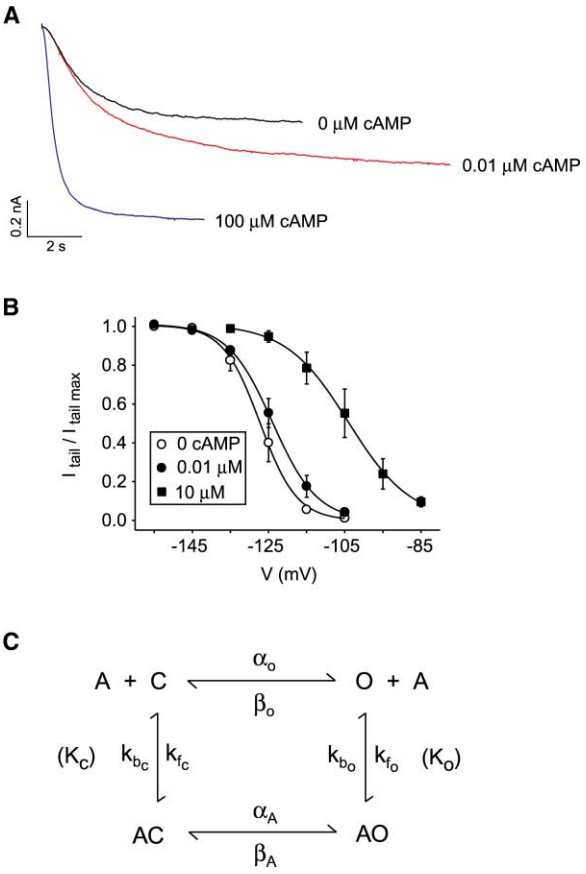

Figure 1. The Steady-State and Kinetic Effects of cAMP Signaling for HCN2

(A) Superimposition of current records from a cell-free inside out-patch in the presence of 0, 0.01, and 100 μM cAMP, in response to voltage steps to −135mV from a holding potential of −40mV for variable durations.

(B) Effect of cAMP on steady-state activation. Normalized tail currents (at −40mV) plotted as a function of hyperpolarizing voltage. Solid lines show fits of the Boltzmann equation. Bars indicate SEM. Open circles, no cAMP, $V_{1/2} = -127$mV, s = 5mV (seven patches); filled circles, 0.01 μM cAMP, $V_{1/2} = -124$mV, s = 6mV (six patches); filled squares, 10 μM cAMP, $V_{1/2} = -104$mV, s = 8mV (five patches).

(C) The cyclic allosteric model for cAMP modulation of HCN gating. α_o and β_o are the first-order, voltage-dependent rate constants for activation and deactivation, respectively, of unliganded channels; α_A and β_A are the voltage-dependent rate constants for the liganded channels. k_{b_c} and k_{f_c} are rates of cAMP unbinding and binding, respectively, to the closed channel. k_{b_o} and k_{f_o} are respective rates for the open channel. K_c and K_o are dissociation equilibrium constants (k_b/k_f) for closed and open states, respectively.

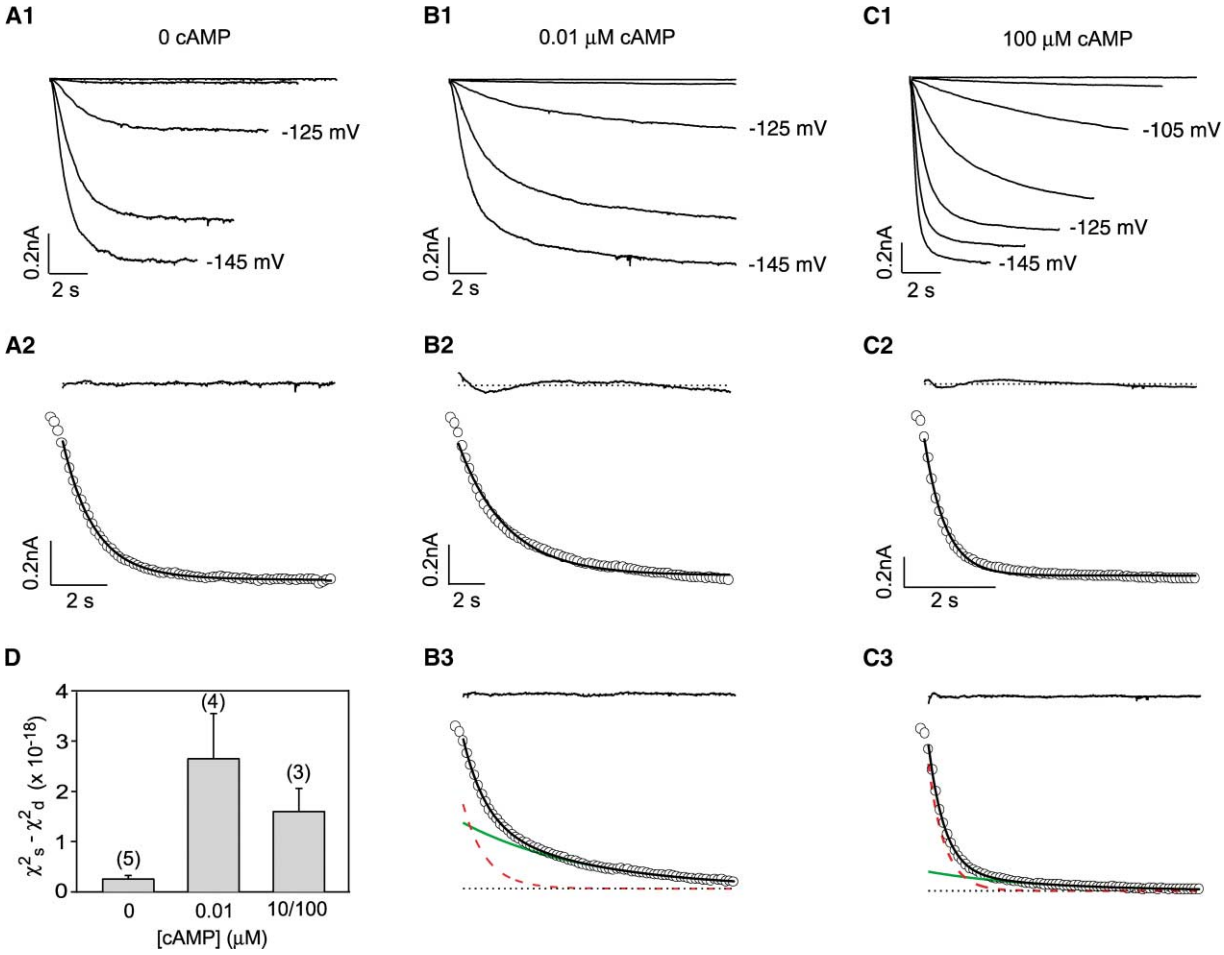

Figure 2. Effect of cAMP on HCN2 Current Kinetics in Cell-free Inside-Out Patches

(A1, B1, and C1) Hyperpolarization-activated currents in response to voltage steps from −85 to −145mV in 10mV increments for variable durations (4.5–15 s) with indicated [cAMP] in the bath solution. Holding potential was −40mV.

(A2, B2, and C2) Bottom, currents recorded at −135mV (open circles) with superimposed single exponential fit (dark line); top, residuals of difference between the data and the fitted curve, with zero residual difference indicated by the dotted lines.

(B3 and C3) Bottom, same currents as above with superimposed double exponential fits; individual fast (red dashed line) and slow (green solid line) exponential components are shown, along with steady-state current (black dotted line); top, residuals of difference between data and fit.

(D) The difference between χ^2_s for single exponential fit and χ^2_d for double exponential fit for current at −135mV. Bars represent SEM. Number of patches given above bars.

are needed to describe the time course of activation in the presence of low concentrations of cAMP (Figure 2B). Thus, fits with a single exponential function show large residuals, and the goodness-of-fit is noticeably enhanced by the addition of a second exponential component (Figure 2D). Moreover, the parameters of the two exponential components are highly reproducible among different patches (see small standard errors in Figure 3). The relatively fast kinetic component has time constants similar to those of the single exponential component for HCN2 channel activation in the absence of cAMP (Figure 3A). Presumably this component represents the direct activation of unliganded, closed channels (C → O). The second, slow exponential component has time constants that are much slower than those in the absence of cAMP. These time constants decrease from ~15 to ~5 s with increasingly negative hyperpolarizations (Figure 3B). Presumably, the slow exponential component represents the slow reequilibration of channels from the unliganded, closed state to the ligand-bound, open state.

At low [cAMP], the relative amplitude of the slow exponential component is large for weak hyperpolarizing steps near the threshold for I_h activation, accounting for up to 80% of the current amplitude. As the voltage step is made more negative, the relative amplitude of the slow component diminishes, accounting for less than 20% of the current amplitude during strong hyperpolarizing steps where activation is maximal (Figure 3C). With increasing concentrations of cAMP, the relative amplitude of the slow component decreases, and the fast and slow time constants accelerate (Figures 3A–3C). At very high concentrations of cAMP, the slow component makes only a minor contribution to the total current amplitude (Figures 2C and 3C).

The voltage and cAMP concentration dependence of the relative amplitudes of the fast and slow exponential components are in good agreement with the cyclic allo-

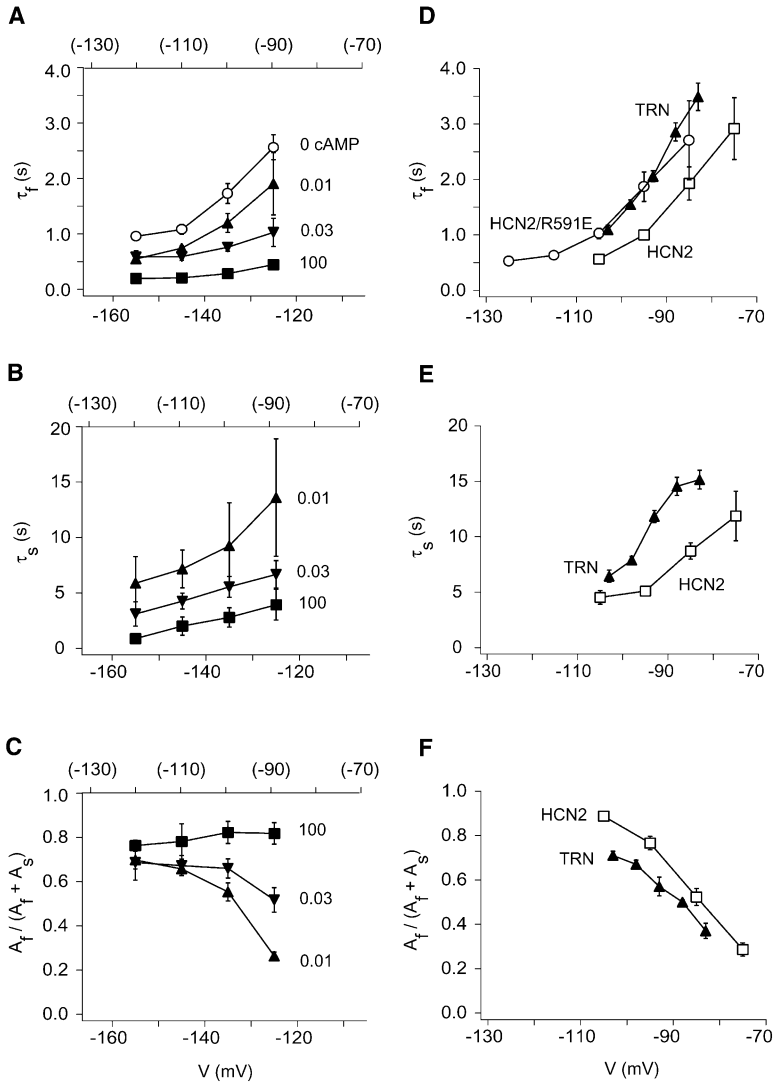

Figure 3. Comparisons of HCN2 Activation Kinetics in Inside-Out Patches and Intact Oocytes with Native I_h of Thalamocortical Relay Neurons (TRN)

(A) Voltage dependence of the fast exponential time constant (τ_f) for currents recorded in the presence of indicated [cAMP] (μM) and of the single exponential time constant for currents measured in the absence of cAMP. (B) Voltage dependence of the slow exponential time constant (τ_s) for patches exposed to indicated [cAMP].

(C) Relative amplitude of the fast exponential component, $A_f/(A_f + A_s)$, as a function of voltage. Each point represents an average of 3–13 patches. Lower *x* axis shows the actual test voltage during recordings; upper *x* axis shows the corresponding voltage in intact cells, where $V_{1/2}$ is shifted by approximately +35mV to compensate for voltage shift upon patch excision (Chen et al., 2001).

(D–F) Kinetic analysis of HCN2 currents in intact oocytes recorded with two-microelectrode voltage clamp and I_h recorded in whole-cell patch clamp from native TRNs. Currents were fit by one or two exponential functions (see Figure 5). Data for HCN2 and HCN2/R591E are averaged from five to nine cells. Data for TRN (recorded at 34°C) are replotted from Santoro et al. (2000) after conversion to expected rates at room temperature using a Q_{10} of 4. (D) Voltage dependence of the fast exponential time constant (τ_f) for HCN2 and TRN and single exponential time constant of HCN2/R591E point mutant. (E) Slow exponential time constant (τ_s) for HCN2 and TRN. HCN2/R591E channels did not display a noticeable slow component (see Figure 5D). (F) Relative amplitude of the fast component for HCN2 and TRN. Bars indicate SEM.

steric model. Thus, a weak hyperpolarization will only open a small fraction of the closed, unliganded channels through the nonfacilitated voltage-gated pathway (C → O). As a result, there will be a large residual population of closed channels that can open through the slow, allosteric reequilibration pathway, generating a large slow phase of activation. In contrast, a strong hyperpolarization will open directly almost all of the closed, unliganded channels through the nonfacilitated voltage-gated pathway, generating a large, relatively rapid component of activation. The decrease in amplitude of the slow phase at high concentrations of cAMP ($>>K_C$) can be explained by the binding of high levels of cAMP to the closed state of the channel. As a result, most channels will exist in the cAMP-bound, closed state (AC) prior to the hyperpolarization, and thus, will activate very rapidly through the facilitated voltage-gated pathway (AC ↔ AO).

The cyclic allosteric model also provides a good quantitative fit to HCN2 activation kinetics, giving us the first estimates for the rate constants of the cAMP binding reaction (Figure 4). We used a nonlinear routine to fit the activation time course for currents elicited at subsaturating cAMP concentrations upon hyperpolarization to four different voltages (see Experimental Procedures) (Figures 1C, 4A, and 4B). Based on fits from three separate experiments, we obtain an average forward rate constant for cAMP binding to the open state (k_{f_o}) of 3.1×10^6 $M^{-1}s^{-1}$ and an average dissociation rate constant for unbinding from the open state (k_{b_o}) of 0.045 s^{-1} (closed state ligand binding kinetics have little influence on I_h kinetics in these experiments and so are not well determined). The fits also yield cAMP equilibrium dissociation constants for binding to the open state (K_O) and closed state (K_C) of ~15 nM and 1.2 μM, respectively.

Basal Levels of cAMP in Intact Cells Induce the Slow Allosteric Conversion

The high affinity of the open channel for cAMP suggests that basal levels of cAMP in intact cells may be sufficient to produce the slow allosteric conversion during prolonged hyperpolarization. Indeed, when we examine the kinetics of HCN2 activation in intact oocytes using a two-microelectrode voltage clamp, we observe a fast

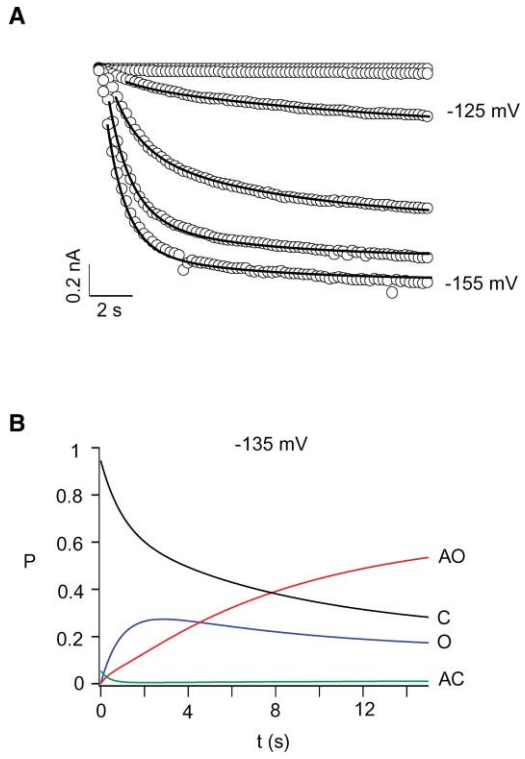

Figure 4. Quantitative Fit of the Cyclic Allosteric Model to HCN2 Currents in a Cell-free Patch with 0.01 μM cAMP

(A) Open circles, current records from Figure 2B; solid lines, superimposed fits with the allosteric model using $k_{f_o} = 2.1 \times 10^6\ M^{-1}s^{-1}$ and $k_{b_o} = 0.045\ s^{-1}$.

(B) Occupancy of four states during hyperpolarization to −135mV according to the fit from (A). Probability (P) as function of time for open cAMP-bound state (AO, red line), closed cAMP-bound state (AC, green line), open unliganded state (O, blue line), and closed unliganded state (C, black line).

and a slow exponential component (Figures 5A, 5C, and 5E) whose properties resemble those of HCN2 in cell-free patches with low concentrations of cAMP (Figure 3). This slow component of HCN2 activation in intact cells, moreover, results from an action of basal levels of cAMP. Thus, when we eliminate cAMP binding to the channel through a point mutation in the CNBD (R591E, which has no effect on voltage gating in the absence of cAMP) (Chen et al., 2001), the slow component of activation is abolished, and channels activate with relatively rapid kinetics that are adequately described by a single exponential function (Figures 5B and 5D). Moreover, the time constants of this fast exponential component recorded at different voltages (Figure 3D) are similar to those recorded for channels in cell-free patches in the absence of cAMP (Figure 3A).

A slow increase in cAMP binding to HCN channels during hyperpolarization, which shifts channels from energetically unfavorable to energetically favorable gating states, also accounts for the striking dependence of $V_{1/2}$ on hyperpolarizing pulse length that has been reported in several previous studies (Seifert et al., 1999; Chen et al., 2001; Ulens and Tytgat, 2001) (Figure 5F). Thus, during relatively short pulses, the opening reaction is largely determined by the more negative voltage dependence of the unliganded channels (C ↔ O). In contrast, the opening equilibrium at the end of prolonged hyperpolarizations, which enable channels to enter the ligand-bound open state, will be determined by the more positive voltage dependence of the ligand-bound channels (AC ↔ AO). HCN2/R591E channels, which do not bind cAMP, show a much faster equilibration of their $V_{1/2}$ values, reflecting only the (relatively rapid) kinetics of the activation reaction for unliganded channels (Figure 5F).

In neurons, the kinetics of I_h channels are also consistent with the induction of the slow allosteric conversion by basal levels of cAMP. Thus, in thalamocortical relay neurons (TRN), which show a high level of expression of HCN2 (Santoro et al., 2000), the time course of I_h activation exhibits both a fast and a slow exponential component (Figures 3D–3F), whose voltage-dependent characteristics resemble the behavior of HCN2 in intact oocytes and in cell-free patches with low concentrations of cAMP. By comparing the activation kinetics of I_h in intact oocytes or thalamocortical relay neurons with the kinetics of I_h in cell-free patches (Figure 3), we estimate that basal levels of cAMP are ~10–40 nM in both types of cells.

Slow Allosteric Conversion by Basal Levels of cAMP Imparts an Activity-Dependent Memory to I_h

The slow rate of dissociation of cAMP from the open state (~$0.045\ s^{-1}$) predicts that I_h should display a significant activity-dependent memory. Thus, in an intact neuron, a prolonged burst of hyperpolarizing inhibitory postsynaptic potentials (IPSPs) should result in the opening of HCN channels, followed by the binding of basal cAMP to the open channel, leading to both fast and slow phases of activation. Once the burst of IPSPs terminates, the channels should persist in the open, ligand-bound state for a prolonged period due to the slow off-rate of cAMP (and the fact that the cAMP-bound channels will tend to remain open at typical neuronal resting potentials of −70mV), generating a prolonged I_h tail current.

We have tested this prediction for HCN2 channels in intact oocytes using a train of hyperpolarizing voltage clamp pulses to mimic a burst of IPSPs (Luthi and McCormick, 1998a) (Figure 6A). This protocol does indeed generate a slow increase in I_h during the hyperpolarizing burst that is followed by a prolonged tail of channel opening, in which I_h requires tens of seconds to decay back to baseline. Moreover, we find that these slow kinetics are due to the slow binding and unbinding of cAMP, and not to the inherent voltage-gated kinetics of the channel, because HCN2/R591E channels, which cannot bind cAMP, fail to display the prolonged tail of channel opening (Figure 6B).

Predicted Effects of Basal Levels of cAMP in a Model Thalamocortical Relay Neuron

In intact neurons, the slow tail of I_h activation should generate a prolonged afterdepolarization following a burst of IPSPs. To evaluate the likely characteristics of this effect, we combined the cyclic allosteric model of I_h with a computer model of the electrophysiological properties of thalamic relay neurons (McCormick and

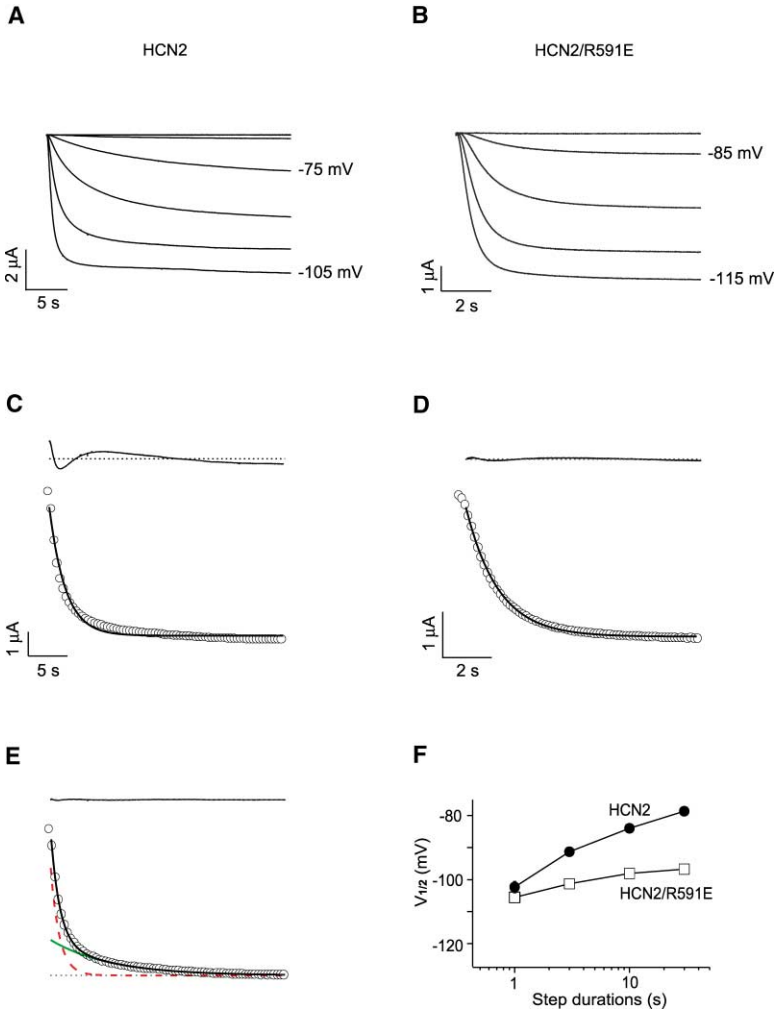

Figure 5. Slow Phase of Activation of HCN2 in Intact *Xenopus* Oocytes Is Eliminated by a Point Mutation that Prevents cAMP Binding

(A) HCN2 hyperpolarization-activated currents from intact oocytes held at −30mV and stepped for 30 s to potentials between −35 and −105mV in 10mV increments.

(B) HCN2/R591E currents during 10 s steps to voltages from −65 to −115mV.

(C and D) Bottom, HCN2 and HCN2/R591E currents during a step to −95mV (open circles) superimposed with a single exponential fit (solid line); top, residual difference between the data and the fit, with zero residual difference indicated by the dotted line.

(E) Bottom, HCN2 current at −95mV (open circles) with superimposed double exponential fit (black solid line) and individual fast (red dashed line) and slow (green solid line) exponential components. Steady-state current is shown as black dotted line. Top, residual difference between data and fit. Fits of HCN2/R591E with a second exponential component either failed to converge or did not yield a significant improvement in χ^2 (data not shown). Time constants and relative amplitudes for fits shown in Figures 3D–3F.

(F) Dependence of $V_{1/2}$ on hyperpolarizing step duration for HCN2 (filled circles, 3 cells) and HCN2/R591E (open squares, 13 cells) channels in intact oocytes. Bars indicate SEM.

Huguenard, 1992; Destexhe et al., 1996). We first studied how cAMP alters the kinetics of membrane potential responses to constant current injection. In the absence of cAMP, negative current steps cause a membrane hyperpolarization followed by a rapid, partial depolarization or "sag," reflecting activation of the inward I_h (Figure 7A). At the end of the current step, a brief rebound afterdepolarization occurs before the membrane potential returns to rest, reflecting the relatively rapid kinetics of I_h deactivation (O → C).

In the presence of 40 nM cAMP, the sag and rebound contain an additional slow phase. The slow phase of the sag reflects the slow component of activation of I_h in low concentrations of cAMP (due to accumulation of channels in the cAMP-bound open state: C → A + O → AO). The slow, persistent phase of the afterdepolarization reflects the persistent tail of I_h activation (due to the slow rate of cAMP dissociation from open channels: AO → O → C). The amplitude and duration of the rebound depolarization increase with the duration of the current step, reflecting increased accumulation of channels in the cAMP-bound, open state (Figures 7A and 7B).

By contrast, in the presence of saturating cAMP, the sag and rebound depolarizations are surprisingly small and rapid, with a duration similar to those observed in the absence of cAMP (Figure 7A). This is because, at high concentrations, cAMP will bind to the closed state of the channel. Moreover, because cAMP-bound channels can open at the resting potential due to their facilitated gating, most I_h channels will exist in the cAMP-bound open state (AO) prior to the hyperpolarizing current pulse. As a result, relatively few closed I_h channels are available to activate during the hyperpolarization pulse (or shut upon termination of the current step), causing a reduction in the size of the depolarizing sag (and subsequent rebound afterdepolarization). In addition, the slow phase of both the sag and rebound depolarization are eliminated because the kinetics are dominated by the facilitated voltage-gating reaction of channels in the cAMP-bound state (AC ↔ AO). These results thus demonstrate the importance of the dynamic allosteric conversion, rather than cAMP per se, for the slow kinetic processes.

The cyclic allosteric model also predicts that a transient increase in cAMP can have long-lasting effects on channel gating that are dependent on the electrical activity of a cell. At membrane potentials where HCN channels are partially open, a brief increase in cAMP concentration leads to a prolonged enhancement of channel activation that persistently depolarizes the

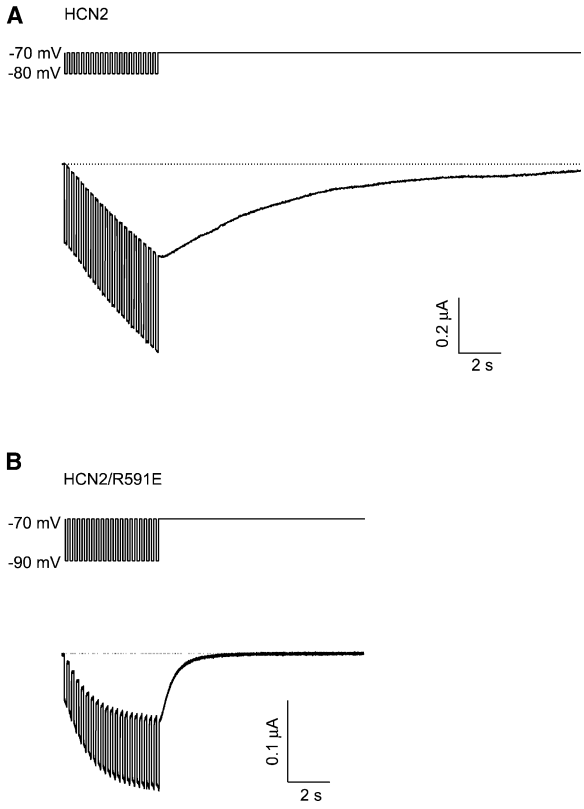

Figure 6. Activity-Dependent Memory of I_h Due to Modulation by Basal Levels of cAMP

(A) Repetitive hyperpolarizations mimicking a burst of IPSPs cause persistent activation of I_h in intact oocytes. HCN2 current (bottom) during and after repetitive hyperpolarizations from −70 to −80mV (top, 20 pulses of 130 ms duration at 4 Hz) is shown. Dotted line shows holding current at −70mV.

(B) HCN2/R591E channels (mutants with an impaired ability to bind cAMP) do not display the slow tail of persistent I_h activation. In this experiment, the membrane was stepped from −70 to −90mV (the more negative step was used to ensure adequate opening of the unliganded channels); otherwise the voltage-clamp protocol was identical to that shown in (A).

membrane long after cAMP has decayed, due to the slow unbinding of cAMP from the open channel (AO → O; Figures 7C and 7 D). However, short, positive current steps applied during the depolarization are able to curtail the depolarization (Luthi and McCormick, 1999) (Figure 7D). This is due to the rapid deactivation of I_h at positive voltages (AO → AC), which leads to the rapid dissociation of cAMP from the low-affinity, closed state of the channel (AC → C + A). This regulation of I_h due to interaction of transient changes in cAMP with membrane voltage is likely to contribute to prolonged voltage changes that occur in thalamocortical neurons during spindling, a form of rhythmic activity found during slow wave sleep (Luthi and McCormick, 1998a, 1998b, 1999).

Discussion

Although cyclic allosteric models have been used previously to explain channel modulation (Bean, 1989; Zagotta and Siegelbaum, 1996), their dynamic implications for slow, activity-dependent processes have been less thoroughly studied. Here we show how low levels of cAMP induce a very slow component of HCN channel activation due to the allosteric coupling of channel opening to enhanced ligand binding. Moreover, the very slow rate of cAMP dissociation endows I_h with an activity-dependent memory that generates a persistent phase of channel opening that lasts for tens of seconds. Such slow modulatory processes, when layered onto the faster kinetics of HCN channel voltage gating, impart a dynamic range to I_h kinetics that can span more than two orders of magnitude. This helps explain how HCN channels underlie both relatively fast rates of spiking at 5–10 Hz and slower periodic oscillations that wax and wane over many seconds (Pape, 1996; Luthi and McCormick, 1998a, 1998b, 1999).

The importance of I_h for neuronal rhythmic activity has been extensively investigated in the thalamus, where it contributes to spindling, a form of synchronized network activity during slow wave sleep, consisting of seconds-long bursts of high frequency oscillations (6–14 Hz) separated by periods of quiescence lasting 5–10 s (Luthi and McCormick, 1998a, 1998b). The long silent period is due to a cumulative build-up of I_h in thalamocortical relay neurons during a burst of hyperpolarizing IPSPs from the inhibitory thalamic reticular neurons, generating a prolonged afterdepolarization that terminates the burst of activity (Steriade et al., 1993; Bal et al., 1995). The slow decay of I_h over several seconds determines the duration of the interburst interval. Luthi and McCormick (1998a, 1998b, 1999) have shown that the slow build-up of I_h is due, in part, to an activity-dependent increase in [cAMP], resulting from the activation of a Ca^{2+}-sensitive adenylate cyclase in response to Ca^{2+} influx during the burst of action potentials. Our data indicate how allosteric coupling will cause I_h channel gating during the burst of IPSPs to enhance cAMP binding, an effect that will synergistically combine with any increase in basal cAMP to further promote channel opening and contribute to the slow periodicity of spindling.

In addition to the physiological implications for neuronal rhythmic activity, our results also suggest a novel mechanism for dynamic signaling through second messenger cascades. To date, most studies have focused on the importance of transient changes in second messenger concentrations, usually caused by transient changes in the concentration of an external ligand, as the driving force behind the dynamics of cellular signal transduction. In contrast, our results show how constant basal levels of cAMP can produce slow, modulatory changes in the electrophysiological properties of excitable cells through the activity-dependent coupling of channel gating to the enhanced affinity of the open channel for its second messenger ligand. Activity-dependent modulation by a time invariant second messenger should be a general feature of cells that express members of the HCN family. In addition, such modulatory processes are also likely to be important for other types of ion channels that are directly regulated by both the binding of an internal second messenger and voltage, including the Ca^{2+}- and voltage-activated Maxi-K^+ channels (Cox et al., 1997), the cyclic nucleotide-regulated and voltage-activated HERG K^+ channels (Cui et

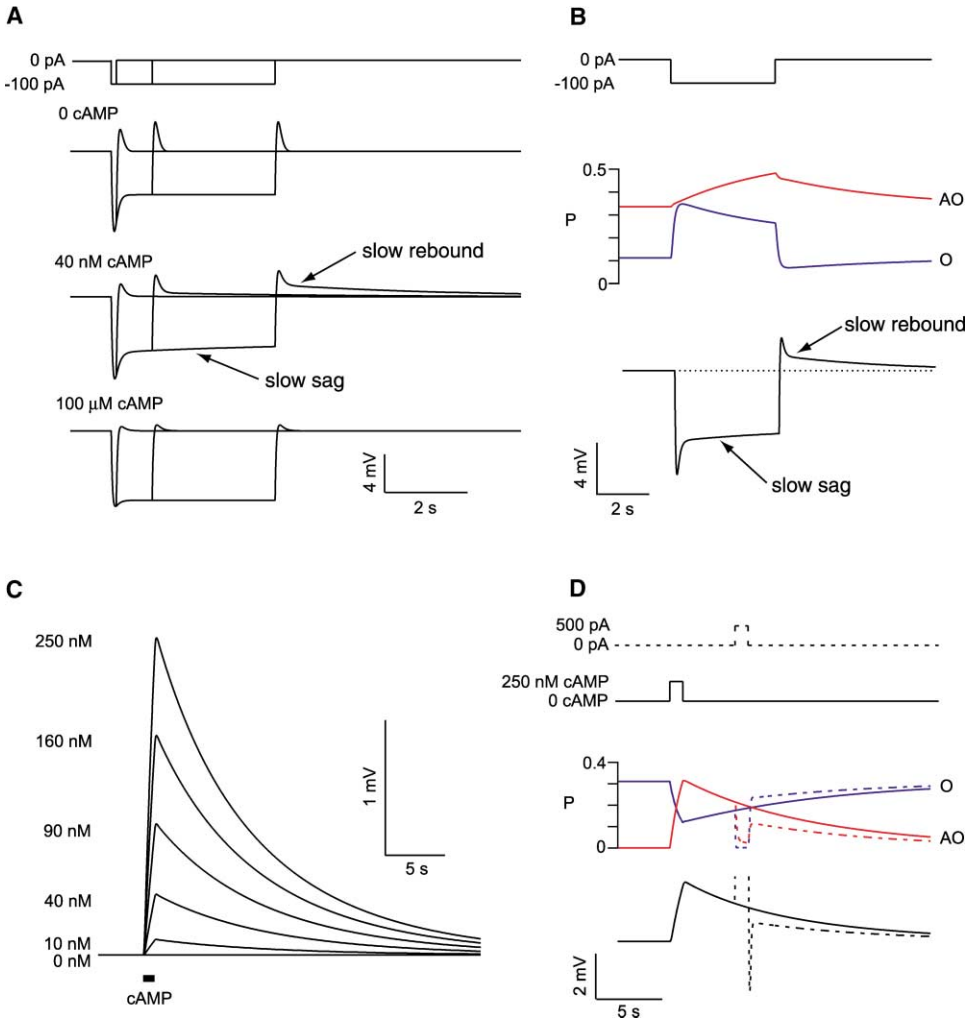

Figure 7. The Physiological Implications of the Cyclic Allosteric Gating Scheme Are Demonstrated in a Computational Model of a TRN

(A) Calculated membrane potential responses to a series of −100 pA current steps (top traces) of increasing duration (0.125, 1, and 4 s) with indicated concentrations of intracellular cAMP. Slow components of the sag and rebound afterdepolarization (arrows) were only observed at the intermediate concentration of cAMP. Calculated resting potentials were −77mV in 0 cAMP, −74mV in 40 nM cAMP, and −68mV in 100 μM cAMP. Similar differences in the sag and rebound were observed when the resting potential was adjusted to the same level in each condition by injection of a constant current (data not shown). (Note: an apparent increase in input resistance with increasing cAMP results from estimating input resistance in current clamp at membrane potentials where voltage-gated channels are active. The apparent increase in input resistance is not found in instantaneous voltage clamp currents during steps from −70 to −75mV. Input resistances of 159, 143, and 102 MΩ were obtained with 0, 0.04, and 100 μM cAMP, respectively.)

(B) Occupancy of open states during a 4 s hyperpolarizing (−100 pA) current step in 40 nM cAMP. A slow transition from the open, unbound state (O, blue line) to the open, cAMP-bound state (AO, red line) causes the slow sag in membrane potential (black traces, bottom). After the pulse ends, channels exit AO very slowly, causing the prolonged rebound depolarization (the channels eventually return to state C via state O). Resting membrane potential (−74mV) is indicated by the dotted line.

(C) Brief (1 s) pulses of increasing concentrations of cAMP (10–250 nM) cause a prolonged (>20 s) depolarization.

(D) The depolarization (bottom, solid black trace) in response to a 250 nM cAMP pulse (upper, solid black trace) is due to an accumulation of channels in the open, cAMP-bound state (AO, solid red lines). A brief depolarizing current step (500 pA for 1 s; upper, black dashed trace) causes a rapid closure of the channels that curtails the depolarization (bottom, black dashed trace). All dashed lines indicate the altered response after the depolarizing step.

al., 2000), and the G protein-regulated, voltage-gated Ca^{2+} channels (Bean, 1989).

Although the simple version of the cyclic allosteric model we have used in this analysis captures a number of key features of how cAMP binding regulates I_h gating, it clearly is an oversimplification. In particular, it does not account for the sigmoidal activation kinetics upon hyperpolarization, in either the absence or the presence of cAMP. Recently, Altomare et al. (2001) modeled the kinetics of I_h activation in the absence of cyclic AMP using a multistate, allosteric activation scheme consistent with the presumed tetrameric structure of the channels. In this model, each individual subunit independently undergoes a voltage-dependent gating transition between a resting and an active state. Each activation reaction enhances the energetics of a single concerted,

allosteric conformational change that opens the channel through a cooperative interaction among all four subunits. Our treatment essentially combines these multiple voltage-gating steps into a single, first-order gating reaction (C ↔ O). Insofar as voltage-gating is rapid relative to cyclic nucleotide binding, a condition that is likely to be met for low concentrations of cAMP, this simplification should not significantly alter the conclusions of our study.

A second simplification concerns the number of cyclic nucleotides that bind to modulate channel gating. At present, there is no direct data concerning the cAMP stoichiometry of I_h channel gating. For the related CNG channels, each channel has been shown to bind up to four molecules of cyclic nucleotide, although binding of fewer than four ligands is sufficient to enhance channel gating (Ruiz and Karpen, 1997; Liu et al., 1998). In the absence of detailed empirical data for HCN channels, we have assumed that there is only a single cyclic nucleotide binding event. Although the presence of multiple ligand binding events would clearly affect the quantitative estimates for rate constants of ligand binding and unbinding, they would not alter our qualitative conclusions that channel gating is allosterically coupled to enhanced ligand binding, and that the enhanced binding to the open state persists for many seconds.

A detailed model based on the multistate activation kinetics of I_h combined with future experimental findings on cAMP stoichiometry will, no doubt, be useful in refining our quantitative picture of HCN channel gating and modulation. However, our present experimental results and analysis provide a clear indication of the important role that the allosteric coupling of channel gating to ligand binding plays in both the action of cAMP to enhance channel activation and in the physiological regulation of cellular and network activity in the central nervous system.

Experimental Procedures

Electrophysiological Recordings

Cell-free inside-out patches were obtained 3–6 days after cRNA injection as previously reported (Wang et al., 2001). The pipette solution contained 107 mM KCl, 5 mM NaCl, 10 mM HEPES, 1 mM $MgCl_2$, and 1 mM EGTA (pH 7.3). The (internal) bath solution contained 104 mM K-Aspartate, 3 mM KCl, 5 mM NaCl, 10 mM HEPES, 1 mM $MgCl_2$, and 1 mM EGTA (pH 7.3). The holding potential was −40mV. Hyperpolarizing voltage steps of variable length (4–15 s) were used. Two microelectrode voltage-clamp recordings were performed 1–2 days after cRNA injection as previously reported (Chen et al., 2001). The recordings were obtained with oocytes bathed in a high KCl solution containing 96 mM KCl, 2 mM NaCl, 10 mM HEPES, and 2 mM $MgCl_2$ (pH 7.5). Microelectrodes were filled with 3 M KCl and had resistances of 0.5–2 MΩ. Holding potential was −30mV. Analysis was done using Pulsefit (HEKA) and IgorPro (WaveMetrics). Linear leak current was not subtracted. All recordings were obtained at room temperature (22°C–25°C).

I_h Current Analysis

Channel Kinetics

Activation curves were fit with either a single exponential ($I = I_{ss} + A\exp[-t/\tau]$) or a double exponential function ($I = I_{ss} + A_f\exp[-t/\tau_f] + A_s\exp[-t/\tau_s]$) after an initial delay (Wainger et al., 2001). I_{ss} represents the steady-state current, and τ represents the time constant. Goodness-of-fit was evaluated using $\chi^2 = \Sigma(x_i - x)^2/x_i$, where x_i is the experimental current value at a given time point and x is the fitted value. For a quantitative analysis of the adequacy of single versus double exponential fits of the time course of I_h activation in the absence and presence of cAMP, we calculated the difference between χ^2 for a single exponential fit and χ^2 for a double exponential fit. To compare χ^2 values at different pulse lengths, these values were divided by the number of points per current record (a constant sampling rate of 1 kHz used for all pulse lengths). In experiments in the absence of cAMP or with saturating cAMP, where channel kinetics are relatively rapid, we used a variable pulse length protocol (DiFrancesco, 1999) that allowed channel activation to approach steady-state values at each voltage but minimized the length of the hyperpolarization to prevent membrane damage during hyperpolarization. In subsaturating cAMP where channel kinetics are slow, we used a 15 s pulse to allow activation to approach steady state. To ensure that the use of different pulse lengths did not influence the exponential fitting procedure, we compared fits using 15 s pulses to fits using shorter pulses (6–10 s) in a subset of experiments (in the absence of cAMP or the presence of saturating cAMP). We observed no difference in the time constants of activation or in the quality of single versus double exponential fits in these experiments. After normalization, there was no significant difference in χ^2 values for fits using different pulse lengths, justifying the use of the variable pulse protocol.

Steady-State Activation

Activation curves were determined from the amplitudes of tail currents measured on return to −40mV after hyperpolarizing steps to different test voltages as previously described (Wang et al., 2001). Tail currents were fit with a modified Boltzmann equation: $I = A_1 + A_2/(1 + \exp[\{V - V_{1/2}\}/s])$, where A_1 is an offset caused by a nonzero holding current, A_2 is the maximal tail current amplitude, V is voltage during the hyperpolarizing test pulse (in mV), $V_{1/2}$ is the midpoint activation voltage, and s is the slope of the relation (in mV). Tail current amplitudes from individual experiments were normalized by subtracting A_1 and dividing by A_2. The normalized data were averaged among the different experiments and refit by the Boltzmann equation with A_1 set to 0 and A_2 set to 1.

Fitting of the Kinetics by the Allosteric Model

We used the model of Figure 1C to fit I_h activation kinetics during hyperpolarizations in the presence of intermediate concentrations of cAMP using the Levenberg-Marquardt nonlinear least squares algorithm of Igor Pro. The model contains four voltage-dependent rate constants for the two voltage-gating reactions and four voltage-independent rate constants for the cAMP binding reactions. Because of the cyclic nature of the model, the rate constant for cAMP dissociation from the closed state, k_{b_c}, was calculated from the other seven rates. Values for the four voltage-dependent rates were partially constrained from experimental measurements of activation time constants in the absence of cAMP, $\tau = 1/(\alpha_O + \beta_O)$, and of the major, fast time constant of activation in the presence of saturating cAMP, $\tau = 1/(\alpha_A + \beta_A)$. Steady-state open probability for the unliganded state, $P_O = \alpha_O/(\alpha_O + \beta_O)$, was a free parameter. Although P_O could have been constrained by our measured value of P_O in the absence of cAMP, a small progressive negative shift in $V_{1/2}$ after patch excision (Chen et al., 2001) led to small shifts in P_O during the experiment. Fitted values of P_O were always within 25% of the actual measured values. Steady-state open probability for the ligand-bound state, $P_{AO} = \alpha_A/(\alpha_A + \beta_A)$, was calculated from the fitted value of P_O and the measured shift in $V_{1/2}$ of the steady-state activation curve in saturating cAMP (~20mV) (Wang et al., 2001). The forward association rate constant for cAMP binding to the closed and open channels, k_{f_c} and k_{f_o}, as well as the rate constant for cAMP dissociation from the open state, k_{b_o}, were free parameters. The time course of activation of I_h for a given set of rate constants was calculated using the Q-Matrix approach (Colquhoun and Hawkes, 1995).

Thalamocortical Neuron Simulations

Thalamocortical relay cells were simulated with a modified version of a previously described single compartment model (McCormick and Huguenard, 1992; Destexhe et al., 1996) using the program Neuron (Hines and Carnevale, 1997, 2000). To focus on the role of I_h, low-threshold calcium currents were not included in the simulations. The kinetic description of I_h included in the model was based on the four state cyclic allosteric model (Figure 1C) using rate constants derived from fits to our experimental data. Transitions between open

Table 1. Rate Constants of Cyclic Allosteric Model for Simulation of Thalamcortical Neuron

	r_o (ms^{-1})	$V_{1/2}$ (mV)	s (mV)
α_o	1.5×10^{-3}	−87.7	−6.45
β_o	2×10^{-2}	−51.7	6.94
α_A	6.7×10^{-3}	−94.2	−13.33
β_A	1.4×10^{-2}	−35.5	6.94

and closed states (C ↔ O and AC ↔ AO) were governed by forward and backward rate constants (α_O, β_O, α_A, β_A) with a voltage dependence described by a two state Boltzmann distribution: $r(V) = r_O/(1 + \exp[-\{V - V_{1/2}\}/s])$, where r(V) is the value of a given rate constant at voltage V. To account for the difference in $V_{1/2}$ for I_h between inside-out patches from *Xenopus* oocytes and intact thalamocortical cells, the $V_{1/2}$ values for each rate constant were increased by 48mV. The parameters used are given in Table 1. The ligand binding reaction between states O and AO was described by $k_{f_o} = 3.086 \times 10^6\ M^{-1}\ s^{-1}$ and $k_{b_o} = 0.04486\ s^{-1}$, based on the fit of the model in Figure 1C to the inside-out patch data. The closed-state dissociation constant, K_C, was set equal to 80 times that of the open-state dissociation constant, K_O, (according to $\Delta V = s\ln(K_C/K_O)$, where ΔV is approximately 20mV). The corresponding on and off rates for cAMP binding to the closed state were reduced and increased, respectively, by $\sqrt{80}$ relative to the corresponding rates for the open state. To adjust the model parameters, which were determined from experiments at ~22°C, to the simulated temperature of 36°C, we assumed a Q_{10} of 4 for voltage-dependent transitions and 1.5 for ligand binding/unbinding.

Acknowledgments

We thank John Riley and Huan Yao for expert technical assistance and Gareth Tibbs, Chris Ulens, Edgar Young, and Brian Wainger for their helpful comments on the manuscript. This work was partly supported by grant NS36658 from the NIH (to S.A.S.) and by the Howard Hughes Medical Institute. J.W. was supported by the MSTP program. M.F.N. was supported by the New York State Research Foundation for Mental Hygiene (Eric R. Kandel, P.I.), and we thank Eric Kandel for his support and advice.

Received: July 30, 2002
Revised: September 9, 2002

References

Altomare, C., Bucchi, A., Camatini, E., Baruscotti, M., Viscomi, C., Moroni, A., and DiFrancesco, D. (2001). Integrated allosteric model of voltage gating of HCN channels. J. Gen. Physiol. *117*, 519–532.

Bal, T., von Krosigk, M., and McCormick, D.A. (1995). Synaptic and membrane mechanisms underlying synchronized oscillations in the ferret lateral geniculate nucleus in vitro. J. Physiol. *483*, 641–663.

Bean, B.P. (1989). Neurotransmitter inhibition of neuronal calcium currents by changes in channel voltage dependence. Nature *340*, 153–156.

Bhalla, U.S., and Iyengar, R. (1999). Emergent properties of networks of biological signaling pathways. Science *283*, 381–387.

Chen, S., Wang, J., and Siegelbaum, S.A. (2001). Properties of hyperpolarization-activated pacemaker current defined by coassembly of HCN1 and HCN2 subunits and basal modulation by cyclic nucleotide. J. Gen. Physiol. *117*, 491–503.

Colquhoun, D., and Hawkes, A.G. (1995). A Q-Matric cookbook: how to write only one program to calculate single-channel and macroscopic predictions for any kinetic mechanism. In Single-Channel Recording, Second Edition, Sakmann, B., and Neher, E., eds. (New York: Plenum Press), pp. 589–633.

Cox, D.H., Cui, J., and Aldrich, R.W. (1997). Allosteric gating of a large conductance Ca-activated K^+ channel. J. Gen. Physiol. *110*, 257–281.

Cui, J., Melman, Y., Palma, E., Fishman, G.I., and McDonald, T.V. (2000). Cyclic AMP regulates the HERG K(+) channel by dual pathways. Curr. Biol. *10*, 671–674.

Davare, M.A., Avdonin, V., Hall, D.D., Peden, E.M., Burette, A., Weinberg, R.J., Horne, M.C., Hoshi, T., and Hell, J.W. (2001). A beta2 adrenergic receptor signaling complex assembled with the Ca^{2+} channel Cav1.2. Science *293*, 98–101.

Destexhe, A., Bal, T., McCormick, D.A., and Sejnowski, T.J. (1996). Ionic mechanisms underlying synchronized oscillations and propagating waves in a model of ferret thalamic slices. J. Neurophysiol. *76*, 2049–2070.

DiFrancesco, D. (1993). Pacemaker mechanisms in cardiac tissue. Annu. Rev. Physiol. *55*, 455–472.

DiFrancesco, D. (1999). Dual allosteric modulation of pacemaker (f) channels by cAMP and voltage in rabbit SA node. J. Physiol. *515*, 367–376.

DiFrancesco, D., and Tortora, P. (1991). Direct activation of cardiac pacemaker channels by intracellular cyclic AMP. Nature *351*, 145–147.

Gauss, R., Seifert, R., and Kaupp, U.B. (1998). Molecular identification of a hyperpolarization-activated channel in sea urchin sperm. Nature *393*, 583–587.

Goulding, E.H., Tibbs, G.R., and Siegelbaum, S.A. (1994). Molecular mechanism of cyclic-nucleotide-gated channel activation. Nature *372*, 369–374.

Hines, M.L., and Carnevale, N.T. (1997). The NEURON simulation environment. Neural Comput. *9*, 1179–1209.

Hines, M.L., and Carnevale, N.T. (2000). Expanding NEURON's repertoire of mechanisms with NMODL. Neural Comput. *12*, 995–1007.

Karpen, J.W., and Rich, T.C. (2001). The fourth dimension in cellular signaling. Science *293*, 2204–2205.

Kaupp, U.B., and Seifert, R. (2001). Molecular diversity of pacemaker ion channels. Annu. Rev. Physiol. *63*, 235–257.

Liu, D.T., Tibbs, G.R., Paoletti, P., and Siegelbaum, S.A. (1998). Constraining ligand-binding site stoichiometry suggests that a cyclic nucleotide-gated channel is composed of two functional dimers. Neuron *21*, 235–248.

Ludwig, A., Zong, X., Jeglitsch, M., Hofmann, F., and Biel, M. (1998). A family of hyperpolarization-activated mammalian cation channels. Nature *393*, 587–591.

Luthi, A., and McCormick, D.A. (1998a). Periodicity of thalamic synchronized oscillations: the role of Ca^{2+}-mediated upregulation of I_h. Neuron *20*, 553–563.

Luthi, A., and McCormick, D.A. (1998b). H-current: properties of a neuronal and network pacemaker. Neuron *21*, 9–12.

Luthi, A., and McCormick, D.A. (1999). Modulation of a pacemaker current through Ca^{2+}-induced stimulation of cAMP production. Nat. Neurosci. *2*, 634–641.

Marx, S.O., Kurokawa, J., Reiken, S., Motoike, H., D'Armiento, J., Marks, A.R., and Kass, R.S. (2002). Requirement of a macromolecular signaling complex for beta adrenergic receptor modulation of the KCNQ1-KCNE1 potassium channel. Science *295*, 496–499.

McCormick, D.A., and Huguenard, J.R. (1992). A model of the electrophysiological properties of thalamocortical relay neurons. J. Neurophysiol. *68*, 1384–1400.

Michel, J.J., and Scott, J.D. (2002). AKAP mediated signal transduction. Annu. Rev. Pharmacol. Toxicol. *42*, 235–257.

Monod, J., Wyman, J., and Changeux, J.P. (1965). On the nature of allosteric transitions: a plausible model. J. Mol. Biol. *12*, 88–118.

Pape, H.C. (1996). Queer current and pacemaker: the hyperpolarization-activated cation current in neurons. Annu. Rev. Physiol. *58*, 299–327.

Robison, G.A., Butcher, R.W., and Sutherland, E.W. (1971). Cyclic AMP. (New York: Academic Press).

Ruiz, M.L., and Karpen, J.W. (1997). Single cyclic nucleotide-gated channels locked in different ligand-bound states. Nature *389*, 389–392.

Santoro, B., and Tibbs, G.R. (1999). The HCN gene family: molecular

basis of the hyperpolarization-activated pacemaker channels. Ann. N.Y. Acad. Sci. *868*, 741–764.

Santoro, B., Liu, D.T., Yao, H., Bartsch, D., Kandel, E.R., Siegelbaum, S.A., and Tibbs, G.R. (1998). Identification of a gene encoding a hyperpolarization-activated pacemaker channel of brain. Cell *93*, 717–729.

Santoro, B., Chen, S., Luthi, A., Pavlidis, P., Shumyatsky, G.P., Tibbs, G.R., and Siegelbaum, S.A. (2000). Molecular and functional heterogeneity of hyperpolarization-activated pacemaker channels in the mouse CNS. J. Neurosci. *20*, 5264–5275.

Seifert, R., Scholten, A., Gauss, R., Mincheva, A., Lichter, P., and Kaupp, U.B. (1999). Molecular characterization of a slowly gating human hyperpolarization-activated channel predominantly expressed in thalamus, heart, and testis. Proc. Natl. Acad. Sci. USA *96*, 9391–9396.

Steriade, M., McCormick, D.A., and Sejnowski, T.J. (1993). Thalamocortical oscillations in the sleeping and aroused brain. Science *262*, 679–685.

Tibbs, G.R., Goulding, E.H., and Siegelbaum, S.A. (1997). Allosteric activation and tuning of ligand efficacy in cyclic-nucleotide-gated channels. Nature *386*, 612–615.

Ulens, C., and Tytgat, J. (2001). Functional heteromerization of HCN1 and HCN2 pacemaker channels. J. Biol. Chem. *276*, 6069–6072.

Wainger, B.J., DeGennaro, M., Santoro, B., Siegelbaum, S.A., and Tibbs, G.R. (2001). Molecular mechanism of cAMP modulation of HCN pacemaker channels. Nature *411*, 805–810.

Wang, J., Chen, S., and Siegelbaum, S.A. (2001). Regulation of hyperpolarization-activated HCN channel gating and cAMP modulation due to interactions of COOH terminus and core transmembrane regions. J. Gen. Physiol. *118*, 237–250.

Zaccolo, M., and Pozzan, T. (2002). Discrete microdomains with high concentration of cAMP in stimulated rat neonatal cardiac myocytes. Science *295*, 1711–1715.

Zagotta, W.N., and Siegelbaum, S.A. (1996). Structure and function of cyclic nucleotide-gated channels. Annu. Rev. Neurosci. *19*, 235–263.